

## Elastic Proton-Proton Scattering at 1.35, 2.1, and 2.9 BeV\*

T. FUJII, G. B. CHADWICK,† G. B. COLLINS, P. J. DUKE,‡ N. C. HIEN,§  
M. A. R. KEMP,‡, AND F. TURKOT

Brookhaven National Laboratory, Upton, New York

(Received July 10, 1962)

As a part of our program to study  $p$ - $p$  collisions at Cosmotron energies, the differential cross sections for elastic scattering were measured at five laboratory angles between  $2.3^\circ$  and  $17^\circ$  for each incident energy. Total elastic cross sections obtained by integration are  $21.4 \pm 1.4$ ,  $17.0 \pm 0.8$ , and  $14.7 \pm 0.7$  mb at 1.35, 2.1, and 2.9 BeV, respectively. The angular distribution as a function of the momentum transfer, exhibits a forward diffraction peak, the width of which shrinks slightly as the incident energy increases. The experimental results were fitted by simple optical model calculations and also compared with the predictions of the composite particle theory of Chew and Frautschi.

### I. INTRODUCTION

PREVIOUS measurements of elastic proton-proton scattering above<sup>1-6</sup> 1 BeV have revealed that the angular distribution is characterized by a predominant forward peak, indicating a diffraction effect due to inelastic processes. Most experimental angular distributions at small angles agree quite well with the optical model prediction for a purely absorbing disk of radius of the order of  $1 F$ .<sup>1-4</sup> However, a short-range phase shift is required to account for the observed smooth tail at large angles.<sup>2,3</sup> Although this seems to indicate the existence of a potential-like interaction, no clear evidence was found for Coulomb-nuclear interference in the small-angle emulsion measurements at<sup>5</sup> 3 and<sup>6</sup> 8.2 BeV. The extrapolated value of the forward scattering amplitude at 3 BeV was compatible with a very small amount, if any, of real potential scattering.<sup>3,5</sup> The integrated elastic cross section<sup>7</sup> decreases monotonically from 24 mb at 1 BeV to 8 mb at 6-8 BeV, while the

total cross section decreases much more slowly from 47 to 42 mb in the corresponding energy range.<sup>8</sup>

Recently, the composite particle theory developed by Chew, Frautschi, and others<sup>9,10</sup> on the basis of the Regge pole hypothesis has given a definite prediction for the high-energy behavior of the diffraction scattering in terms of energy and momentum variables. Their prediction was consistent with the recent result of Cocconi *et al.*<sup>11</sup> for elastic proton-proton scattering at 13-28 BeV/ $c$ , in which an extremely rapid decrease of the differential cross section at large momentum transfers was observed.

In the light of this new development, an accurate measurement of elastic scattering in the range of momentum transfers less than 1 BeV/ $c$  and at different energies is of interest. In this paper, we report the measurement of the elastic angular distributions at three Cosmotron energies; the experiment utilized the external beam and a liquid-hydrogen target. Since the experiment was primarily designed to study the inelastic part of  $p$ - $p$  collisions,<sup>12</sup> measurements were carried out in a somewhat limited angular range. Nevertheless, our data covered the momentum transfer range of interest ( $0.2$ - $5 F^{-1}$ ) and were free from the complications which were inherent to some of the earlier work using an internal beam and a compound target.<sup>1,2</sup>

### II. EXPERIMENTAL PROCEDURE AND RESULTS

The details of the experimental procedure and the method of data reduction are thoroughly discussed in the preceding paper.<sup>12</sup> We will briefly describe here only

\* Work performed under the auspices of the U. S. Atomic Energy Commission.

† Present address: The Clarendon Laboratory, University of Oxford, England.

‡ On leave from the National Institute for Research in Nuclear Science, Harwell, England.

§ Present address: Department of Physics, Carnegie Institute of Technology, Pittsburgh, Pennsylvania.

<sup>1</sup> L. W. Smith, A. W. McReynolds, and G. Snow, *Phys. Rev.* **97**, 1186 (1955). For the analysis of this work, see R. Serber and W. Rarita, *ibid.* **99**, 629 (1955); and W. Rarita, *ibid.* **104**, 221 (1956).

<sup>2</sup> B. Cork, W. A. Wenzel, and C. W. Causey, *Phys. Rev.* **107**, 859 (1957).

<sup>3</sup> G. A. Smith, H. Courant, E. C. Fowler, H. Kraybill, J. Sandweiss, and H. Taft, *Phys. Rev.* **123**, 2160 (1961).

<sup>4</sup> W. F. Fickinger, E. Pickup, D. K. Robinson, and E. O. Salant, *Phys. Rev.* **125**, 2082 (1962).

<sup>5</sup> W. M. Preston, R. Wilson, and H. C. Street, *Phys. Rev.* **118**, 579 (1960).

<sup>6</sup> S. A. Azimov, B. P. Bannik, V. G. Grishin, Do In Seb, L. F. Kirillova, P. K. Markov, V. A. Nikitin, L. G. Popova, I. N. Silin, L. V. Silvestrov, E. N. Tsyganov, M. G. Shafranov, B. A. Shahbazyan, A. A. Yuldashev, A. Zlateva, A. Peieva, L. Khristov, and Ch. Chernev, *Proceedings of the 1960 Annual International Conference on High-Energy Physics at Rochester* (Interscience Publishers, Inc., New York, 1960), p. 91.

<sup>7</sup> In addition to references 1-6, see W. B. Fowler, R. P. Shutt, A. M. Thorndike, W. L. Whittmore, V. T. Cocconi, E. Hart, M. M. Block, and E. M. Harth, *Phys. Rev.* **103**, 1484 (1956); R. M. Kalbach, J. J. Lord, and C. H. Taso, *ibid.* **113**, 325 (1959).

<sup>8</sup> E. F. Chen, C. P. Leavitt, and A. M. Shapiro, *Phys. Rev.* **103**, 211 (1956); G. Von Dardel, D. H. Frisch, R. Mermod, R. H. Milburn, P. A. Piroué, M. Vivargent, G. Weber, and K. Winter, *Phys. Rev. Letters* **5**, 333 (1960); M. L. Longo and B. J. Moyer, *Phys. Rev.* **125**, 701 (1962).

<sup>9</sup> G. F. Chew and S. C. Frautschi, *Phys. Rev.* **123**, 1478 (1961); *Phys. Rev. Letters* **7**, 394 (1961); **8**, 41 (1962).

<sup>10</sup> S. C. Frautschi, M. Gell-Mann, and F. Zachariasen, *Phys. Rev.* **126**, 2204 (1962).

<sup>11</sup> G. Cocconi, A. N. Diddens, E. Lillethun, G. Manning, A. E. Taylor, T. G. Walker, and A. M. Wetherell, *Phys. Rev. Letters* **7**, 450 (1961).

<sup>12</sup> G. B. Chadwick, G. B. Collins, P. J. Duke, T. Fujii, N. C. Hien, M. A. R. Kemp, and F. Turkot, preceding paper [*Phys. Rev.* **128**, 1823 (1962)].

those features pertinent to the measurement of elastic scattering.

The external proton beam from the Cosmotron was focused at the center of a liquid-hydrogen target within a circle of diameter 2 cm and with an angular divergence of  $\frac{1}{2}^\circ$ . Scattered protons were momentum analyzed by a magnetic spectrometer and detected by four contiguous counter telescopes. For measuring the elastic part of the spectrum, the beam was reduced by factors of 3 to 10 from the full intensity ( $0.5\text{--}2.0 \times 10^{10}$  per pulse) in order to keep counting losses below 1%. The main source of background came from the Mylar windows of the hydrogen target and amounted to a maximum of 10% of the target-full counting rate under the elastic peak. A typical momentum spectrum thus obtained is shown in Fig. 1. The over-all momentum resolution, given by the full width at half-maximum of the elastic peak, varied from 2.2 to 2.9%.

The elastic differential cross section  $(d\sigma/d\Omega)_{\text{lab}}$  at each angle and energy was obtained by integrating the area under the peak. In most of the spectra, the elastic peak was clearly separated from the high-energy tail of the inelastic continuum as seen in Fig. 1. The uncertainty in evaluating the exact height and shape of the peak was examined by comparing the integrated value with that obtained by adding the counts of contiguous counters in the appropriate momentum range. The error in the integration due to these causes was estimated to be less than 2%. The standard deviation attached to the elastic cross section reflects this uncertainty as well as that in the absolute value of  $d^2\sigma/d\Omega dp$  (6–7%) as discussed in the preceding paper.<sup>12</sup>

Table I summarizes all measured elastic cross sections in the laboratory system and in the center of mass system. The quantity  $(1/k^2)(d\sigma/d\Omega)$  is also given as a function of the momentum transfer  $2k \sin(\theta/2)$ , where  $d\sigma/d\Omega$ ,  $\theta$ , and the wave number  $k$  refer to the c.m. system. The spread in the incident beam energy and the

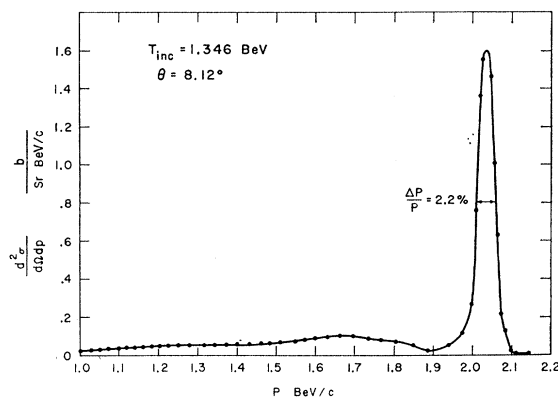


FIG. 1. A typical momentum spectrum of secondary protons at  $8.12^\circ$  for the incident energy 1.35 BeV.

lab angle are  $\pm 0.01$  BeV and  $\pm 0.30^\circ$ , respectively. The latter includes the effect due to the finite size of the target and the divergence of the incident beam.

The angular distributions at the three different energies are shown as a function of the momentum transfer in Fig. 2. It is evident that the data at all energies follow a typical diffraction curve, which decreases by a factor of 10 as the momentum transfer increases from 0 to  $3 \text{ F}^{-1}$ . In the forward direction, all points tend to converge to a nearly identical value, close to the lower limit allowed by the optical theorem; viz.  $(\sigma_T/4\pi)^2$  where  $\sigma_T$  is the total cross section. In the momentum transfer range larger than  $1 \text{ F}^{-1}$ , however, it should be noted that there is a slight but significant decrease in the width of the diffraction peak as the incident energy increases from 1.35 to 2.9 BeV.

The total elastic cross section at each energy was obtained by integrating the experimental angular distribution in the c.m. system. The contribution from the angular range larger than the maximum measured angle was estimated by assuming the cross section

TABLE I. Elastic cross sections in  $p$ - $p$  collision.

$T_{\text{inc}}$ (BeV)	Laboratory system			Center-of-mass system				
	$\theta_{\text{lab}}$ (deg)	$(d\sigma/d\Omega)_{\text{lab}}$ (mb/sr)	$\theta$ (deg)	$d\sigma/d\Omega$ (mb/sr)	$k$ ( $\text{F}^{-1}$ )	$2k \sin(\theta/2)$ ( $\text{F}^{-1}$ )	$(1/k^2)(d\sigma/d\Omega)$ ( $\text{mb}^2/\text{sr}$ )	
1.355	2.37	153 $\pm$ 11	6.22	22.4 $\pm$ 1.6	4.041	0.438	13.7	$\pm$ 1.0
1.351	3.38	147 $\pm$ 10	8.87	21.5 $\pm$ 1.5	4.035	0.624	13.2	$\pm$ 0.9
1.346	8.12	87.4 $\pm$ 6.1	21.18	13.23 $\pm$ 0.93	4.027	1.480	8.17	$\pm$ 0.57
1.329	12.03	50.8 $\pm$ 3.6	31.13	8.08 $\pm$ 0.57	4.001	2.147	5.05	$\pm$ 0.35
1.337	17.35	15.8 $\pm$ 1.1	44.48	2.73 $\pm$ 0.19	4.014	3.039	1.70	$\pm$ 0.12
2.064	2.74	241 $\pm$ 17	7.93	28.9 $\pm$ 2.0	4.987	0.689	11.6	$\pm$ 0.8
2.096	4.17	206 $\pm$ 15	12.11	24.6 $\pm$ 1.7	5.025	1.060	9.76	$\pm$ 0.68
2.066	8.43	82.3 $\pm$ 5.7	24.23	10.39 $\pm$ 0.72	4.989	2.094	4.17	$\pm$ 0.29
2.065	12.00	22.6 $\pm$ 1.6	34.24	3.01 $\pm$ 0.21	4.988	2.937	1.21	$\pm$ 0.09
2.081	17.33	4.79 $\pm$ 0.34	48.77	0.718 $\pm$ 0.050	5.007	4.134	0.287	$\pm$ 0.020
2.868	2.72	386 $\pm$ 27	8.64	38.5 $\pm$ 2.7	5.878	0.886	11.1	$\pm$ 0.8
2.867	4.51	235 $\pm$ 17	14.29	24.1 $\pm$ 1.7	5.877	1.462	6.98	$\pm$ 0.49
2.869	8.53	42.5 $\pm$ 3.0	26.82	4.55 $\pm$ 0.32	5.880	2.727	1.31	$\pm$ 0.09
2.858	12.17	9.67 $\pm$ 0.68	37.81	1.12 $\pm$ 0.09	5.868	3.803	0.324	$\pm$ 0.023
2.897	17.75	0.68 $\pm$ 0.12	54.14	0.227 $\pm$ 0.016	5.908	5.377	0.0649	$\pm$ 0.0045

TABLE II. Optical model parameters for pure absorbing disk.

$T_{\text{inc}}$ (BeV)	$R$ (F)	$1-a$	$\sigma_e^a$ (mb)	Measurement
1.35	$0.87 \pm 0.02$	$0.966 \pm 0.016$	$21.4 \pm 1.4$	this exp.
2.0	0.90	...	$19.21 \pm 0.48$	reference 4
2.07	$0.945 \pm 0.015$	$0.801 \pm 0.013$	$17.0 \pm 0.8$	this exp.
2.25	0.931	0.791	$17 \pm 3$	reference 2
2.85	0.95	0.76	$15.32 \pm 0.76$	reference 3
2.86	$0.995 \pm 0.025$	$0.721 \pm 0.013$	$14.7 \pm 0.70$	this exp.
4.40	1.015	0.556	$10 \pm 2$	reference 2
6.15	1.072	0.470	$8 \pm 2$	reference 2

<sup>a</sup> Obtained by integrating the experimental cross sections.

varied as  $\cos\theta$  in that region. This amounted to 10, 7, and 3% of the total value at 1.35, 2.1, and 2.9 BeV, respectively. Extrapolation to zero angle was made by using the optical model fit to be described in the following section. The values of the total elastic cross section<sup>13</sup> thus estimated are listed in the fourth column of Table II.

We would like to point out an interesting empirical relationship that exist between the elastic data presented here and the inelastic data presented in the preceding article<sup>12</sup>; viz., at the same incident energy the c.m. angular distribution of the elastic scattering is remarkably similar to that of the inelastic cross section at the  $\frac{3}{2}, \frac{3}{2}$  isobar peak in the range between  $8^\circ$  and  $30^\circ$ . This similarity is exhibited in Fig. 3, where the inelastic data was normalized to agree with the elastic data at small angles. Although the elastic distribution generally

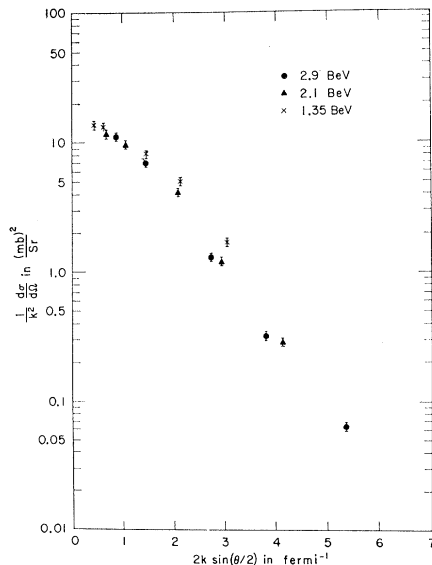


FIG. 2. The elastic angular distributions in the c.m. system at 1.35, 2.1, and 2.9 BeV as a function of the momentum transfer  $2k \sin(\theta/2)$ .

<sup>13</sup> As a result of more careful re-evaluation of the integral over the elastic peak, the corresponding values reported earlier in Bull. Am. Phys. Soc. 7, 45 (1962) should be increased by about 3%.

falls faster at the large angles, the implied relationship is, to a fair approximation, of the form

$$\left(\frac{d\sigma}{d\Omega}\right)_{\text{elastic}}(\theta_{\text{c.m.}}) \simeq C \left(\frac{d^2\sigma}{d\Omega d\rho}\right)_{\text{inelastic}}(\theta_{\text{c.m.}}, \rho_{33}),$$

where  $C$  is 0.59, 0.53, and 0.63 at 1.35, 2.1, and 2.9 BeV, respectively, if  $\rho$  is expressed in BeV/ $c$ . If one separates the inelastic cross section into the unexcited and decay components as discussed in the preceding paper,<sup>12</sup> the relationship persists since the unexcited component is approximately constant at 50% of the total at the  $\frac{3}{2}, \frac{3}{2}$  peak. We also note that the similarity does not hold for an arbitrary point of the inelastic spectrum; e.g., if one chooses the cross section at the momentum corresponding to the 1.52-BeV nucleon isobar, it is no longer true.

### III. DISCUSSION

In order to interpret the angular distribution at each energy, simple optical model calculations<sup>1-4</sup> were carried out. For this model the scattering amplitude is given by

$$f(\theta) = ik \int_0^\infty (1 - ae^{i\phi}) J_0(2k\rho \sin(\theta/2)) \rho d\rho, \quad (1)$$

where  $a$  is the amplitude of the transmitted wave for a unit incident wave and  $\phi$  is the phase shift between the two waves. Both quantities can be chosen to be a particular function of a radius parameter, depending on the type of model assumed.

For small scattering angles, a purely absorbing sphere of radius  $R$  was adopted. With  $a = \text{const}$  for  $\rho \leq R$ , and 0 for  $\rho > R$ , and  $\phi = 0$  everywhere, the elastic differential cross section can be written in the form:

$$\begin{aligned} \frac{1}{k^2} \frac{d\sigma}{d\Omega} &= R^4 (1-a)^2 \left[ \frac{J_1(2kR \sin(\theta/2))}{2kR \sin(\theta/2)} \right]^2 \\ &= \left(\frac{\sigma_T}{4\pi}\right)^2 4 \left[ \frac{J_1(2kR \sin(\theta/2))}{2kR \sin(\theta/2)} \right]^2. \end{aligned} \quad (2)$$

Since the scattering amplitude is assumed to be purely imaginary the equality in the second line holds by definition and is to be justified by the fit to the experimental points in the forward direction.

It is obvious with this model that the shape of the diffraction scattering is determined only by  $R$  while the amplitude is determined by both  $R$  and  $a$ . By adjusting both parameters, a good fit was obtained for all points at 1.35 BeV as shown in Fig. 4(a). The values of the parameters for the best fit were determined as  $R = 0.87 \pm 0.02$  F and  $1-a = 0.966 \pm 0.016$  by using the least-squares method. The uncertainty attached to each parameter corresponds to the variation necessary to increase the value of  $\chi^2$  by 1 from the minimum value

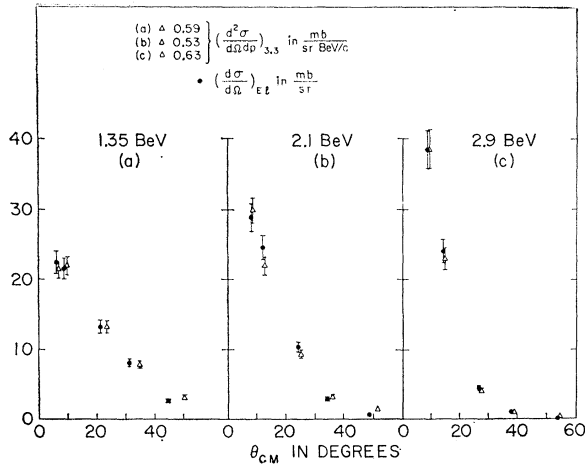


FIG. 3. Comparison of angular distribution between elastic cross sections and inelastic cross sections for producing 1.23-BeV isobar at (a) 1.35, (b) 2.1, (c) 2.9 BeV.

2.1 (expected value 3). The value of the total cross section obtained by extrapolating the best fit and using Eq. (2) is  $46.0 \pm 1.2$  mb, which agrees well with  $46.4_{-0.7}^{+1.5}$  mb, the interpolated value of the transmission measurement by Longo and Moyer.<sup>8</sup>

Similar attempts were made to fit the 2.1- and 2.9-BeV data with this model. Although good fits were obtained for the momentum transfer up to  $3 \text{ F}^{-1}$ , a few points beyond the first diffraction minimum are not compatible with this type of calculations. [See dotted curves in Figs. 4(b) and (c).] In order to account for the discrepancy, the model was modified with a short-range phase shift as described by Cork *et al.*,<sup>2</sup> namely,  $a = \text{const}$  for  $\rho \leq R_2$ ,  $\phi = \text{const}$  for  $\rho \leq R_1$ , and  $\phi = 0$  for  $\rho > R_1$  in Eq. (1). For simplicity,  $R_1$  was chosen about half of  $R_2$  and for each set of chosen values of  $R_1$  and  $R_2$  the values of  $a$  and  $\phi$  were determined so as to be consistent with the measured total elastic and inelastic cross sections<sup>14</sup> by the following equations:

$$\begin{aligned} \text{Elastic, } \sigma_e &= 2\pi \int_0^\infty |(1 - ae^{i\phi})|^2 \rho d\rho; \\ \text{Inelastic, } \sigma_a &= 2\pi \int_0^\infty (1 - a^2) \rho d\rho. \end{aligned} \quad (3)$$

The smooth variation at the large momentum transfer is reasonably well described by this modified model as indicated by the solid curves in Figs. 4(b) and (c).

It is evident that the fit at small angles is rather insensitive to the type of model chosen. Extrapolation using the purely absorbing model gives a forward scattering amplitude corresponding to  $\sigma_T = 44.9 \pm 0.5$  and  $44.8 \pm 2.0$  mb at 2.1 and 2.9 BeV, respectively. These are again close to  $44.7_{-0.4}^{+0.8}$  and  $43.0 \pm 0.6$  mb,

the values measured by Longo and Moyer at those energies. Even if the slight difference between the minimum value and the value obtained by extrapolating a short-range phase shift model is taken seriously, the real scattering amplitude is probably not more than 9% of the imaginary part at 2.9 BeV. This is consistent with the previous results obtained at 3 BeV.<sup>3,5</sup> The contribution of pure Coulomb scattering<sup>15</sup> at the smallest measured angle is estimated to be 1.3, 0.2, and 0.09% at 1.35, 2.1, and 2.9 BeV, respectively.

The optical model parameters obtained with a purely absorbing sphere are listed in Table II and compared with those previously reported<sup>1-4</sup> in this energy range. On the basis of this model, the nucleon becomes more extended and less opaque as the incident energy increases. The effects of increasing radial parameter and decreasing opacity almost cancel each other to account for the slowly varying behavior of the total cross section, given by  $2\pi R^2(1-a)$ , while the total elastic cross section  $\pi R^2(1-a)^2$  is more sensitive to the effect of decreasing opacity.

As mentioned in Sec. I, a completely new approach to high-energy scattering has recently been proposed on the basis of the "composite particle exchange." According to this theory, the scattering amplitude at high energy is governed by the trajectories of particular Regge poles which have appropriate quantum numbers for the interaction. In the case of elastic nucleon-nucleon scattering, Chew and Frautschi,<sup>9</sup> and Frautschi, Gell-Mann, and Zachariasen<sup>10</sup> have predicted the behavior of high energy cross section in the following form:

$$\frac{1}{\pi} \frac{d\sigma}{dt} = \frac{1}{k^2} \frac{d\sigma}{d\Omega} \rightarrow F(t) \left( \frac{S}{2M^2} \right)^{2L_1(t)-2}, \quad (4)$$

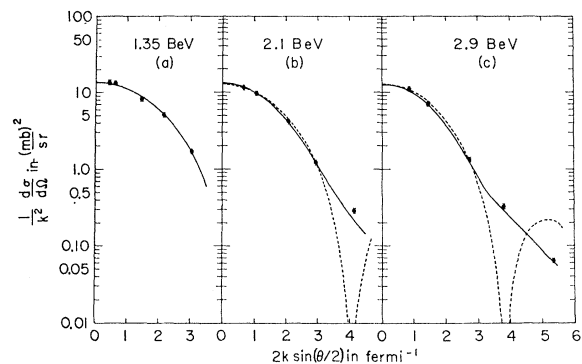


FIG. 4. Optical model fits to elastic angular distributions. (a) 1.35 BeV: Purely absorbing sphere model with  $R = 0.87 \text{ F}$  and  $1-a = 0.966$ . (b) 2.1 BeV: The solid curve represents a short-range phase shift model with  $R_1 = 0.6 \text{ F}$ ,  $R_2 = 1.2 \text{ F}$ ,  $a = 0.653$  and  $\phi = 1.35$  rad. The broken curve represents a purely absorbing sphere model with  $R = 0.945 \text{ F}$  and  $1-a = 0.801$ . (c) 2.9 BeV: The solid curve represents a short-range phase shift model with  $R_1 = 0.56 \text{ F}$ ,  $R_2 = 1.26 \text{ F}$ ,  $a = 0.662$  and  $\phi = 1.27$  rad. The broken curve represents a purely absorbing sphere model with  $R = 0.995 \text{ F}$  and  $1-a = 0.721$ .

<sup>14</sup> Experimental value was obtained from  $\sigma_a = \sigma_{\text{tot}} - \sigma_{\text{el}}$ .

<sup>15</sup> The formula for a point charge proton was used.

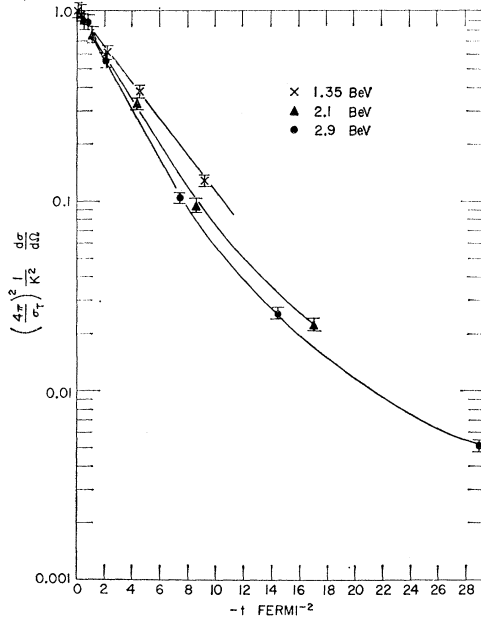


FIG. 5. The angular distribution at 1.35, 2.1, and 2.9 BeV as a function of  $t = -2k^2(1 - \cos\theta)$ .

where  $t = -2k^2(1 - \cos\theta)$  is the negative square of the four-momentum transfer,  $S$  the energy variable  $2M(2M + T_{\text{lab}})$ , and  $L_1(t)$  the variable angular momentum attached to the Regge trajectory corresponding to the quantum numbers of the vacuum. In the physical region,  $t$  is always negative and  $L_1(t)$  is supposed to be less than 1. Hence, this cross section  $(1/k^2)(d\sigma/d\Omega)$  should decrease exponentially with  $|t|$  and the width of the forward peak should shrink logarithmically with increasing energy.<sup>9</sup> Such a tendency was observed experimentally when the elastic differential cross sections measured at 13–28 BeV by Cocconi *et al.*<sup>11</sup> were compared with those<sup>2,3</sup> in the few BeV region for the momentum transfer range  $|t| > 13 \text{ F}^{-2}$ .<sup>12</sup> Using their data in the region  $|t| < (1 \text{ BeV})^2 (26 \text{ F}^{-2})$ , Frautschi *et al.* estimated the rate of change of  $L_1(t)$  to be about  $1/40m_\pi^2$ .<sup>10</sup>

It is not clear whether the energy of our experiment was sufficiently high to apply Eq. (4). However, the fact that we observed a shrinkage of the diffraction peak even in the small momentum transfer range ( $|t| < 20 \text{ F}^{-2}$ ) encouraged us to see if such a simple relation could be used to describe the behavior of the cross sections at these energies.

Figure 5 shows the data at the three energies as a function of  $t$ . The cross section  $(1/k^2)(d\sigma/d\Omega)$  at each energy was divided by  $(\sigma_T/4\pi)^2$  in order to normalize for the slight variation in the total cross section over this energy range. For the range of  $|t|$  less than  $10 \text{ F}^{-2}$ , the experimental points fall off exponentially with a slightly different slope for each energy. It was found by a least-squares fit that the slopes are  $-(0.221 \pm 0.007)$ ,  $-(0.268 \pm 0.007)$ ,  $-(0.301 \pm 0.009) \text{ F}^2$  for 1.35, 2.1, and

2.9 BeV, respectively. The value of 2.9 BeV is very close to that reported by Cocconi *et al.*,<sup>11</sup> who give

$$\begin{aligned} \left(\frac{4\pi}{\sigma_T}\right)^2 \frac{1}{k^2} \frac{d\sigma}{d\Omega} &= e^{-7.5|t|} \quad (t \text{ in BeV}^2) \\ &= e^{-0.29|t|} \quad (t \text{ in F}^{-2}) \end{aligned}$$

for the average of all previous measurements in the range of  $|t|$  less than  $0.5 \text{ BeV}^2 (13 \text{ F}^{-2})$ .

In order to account for the different slopes, we assume a dependence given by<sup>16</sup>

$$\left(\frac{4\pi}{\sigma_T}\right)^2 \frac{1}{k^2} \frac{d\sigma}{d\Omega} = F(t) \left(\frac{S}{4M^2}\right)^{2L(t)-2}, \quad (5)$$

and further assume, for small  $t$ ,

$$L(t) = 1 + \epsilon t.$$

Then,

$$y(S, t) \equiv \left(\frac{4\pi}{\sigma_T}\right)^2 \frac{1}{k^2} \frac{d\sigma}{d\Omega} = F(t) \left(\frac{S}{4M^2}\right)^{-2\epsilon|t|}. \quad (5')$$

To evaluate  $\epsilon$ , we adopted two methods. The first one is simply to take the ratio of the experimental values (or interpolated values)

$$y(S_1, t)/y(S_2, t) = (S_1/S_2)^{-2\epsilon|t|} \quad (6)$$

at  $t = 8 \text{ F}^{-2}$ . The average of two independently estimated values gives  $\epsilon = 0.107 \pm 0.017 \text{ F}^2$ . In the second method, it was assumed that  $F(t)$  also changes exponentially in the range  $|t| \leq 10 \text{ F}^{-2}$ , viz.,  $F(t) = e^{-b|t|}$ . Then,

$$a_i = b + 2\epsilon \ln(S_i/4M^2), \quad (7)$$

where  $a_i$  is the slope of the exponential behavior of  $y(S_i, t)$ , as determined previously. Using the least-squares method, we obtained  $\epsilon = 0.104 \pm 0.014 \text{ F}^2$  and  $b = 0.11 \pm 0.02 \text{ F}^2$ . Both methods seem to indicate that our data is consistent with  $\epsilon = 0.1 \text{ F}^2 = 1/20m_\pi^2$ .

Using this value of  $\epsilon$ , we have plotted the function

$$F(t) = \left(\frac{4\pi}{\sigma_T}\right)^2 \frac{1}{k^2} \frac{d\sigma}{d\Omega} \left(\frac{S}{4M^2}\right)^{2\epsilon|t|}$$

to see if this is a function only of  $t$ . Figure 6 shows the result. The experimental points at three different energies indeed exhibit a smooth variation with  $t$ . The solid line is  $e^{-0.11|t|}$  as given by the second method described above. Although it fits well at small  $t$ , the experimental points decrease more slowly in the range  $|t| > 10 \text{ F}^{-2}$ .

The value of  $\epsilon$  obtained from our data at small

<sup>16</sup> As already mentioned in reference 10, the choice of the factor  $1/4M^2$  in this equation is arbitrary. We normalized  $S$  to its minimum value  $4M^2$ , while Frautschi *et al.* uses the term  $S/2M^2$ . Since any multiplicative constant raised to the power of  $2L(t) - 2$  can be absorbed in  $F(t)$ , the functional form of  $F(t)$  obtained from the experiment also depends on this arbitrary choice.

momentum transfers is about twice the value estimated on the basis of the high-energy scattering data of Cocconi *et al.* at large momentum transfers. Furthermore, if one takes the ratio of our 2.9-BeV data to the 18.7-BeV/c data of Cocconi *et al.* at  $|t| \sim 1.1 \text{ BeV}^2$ , one obtains the slope  $\epsilon = 1/53m_\pi^2 \pm 20\%$ , which is close to the value reported by Frautschi *et al.* A similar plot of  $F(t)$  using  $\epsilon = 1/40m_\pi^2$ , as shown in Fig. 7, provides a fairly good agreement among our data, those of Cork *et al.* and those of Cocconi *et al.* for the range of momentum transfer  $|t| \geq 10 \text{ F}^2$ . If the slope of Regge vacuum trajectory is constant in the region of  $|t| \leq 1 \text{ BeV}^2$ , the discrepancy mentioned above may imply that contributions from  $I=0$  Regge trajectories other than the vacuum line are still substantial in our energy range, where  $S/4M^2$  is of the order of 2. It has been suggested<sup>17</sup>

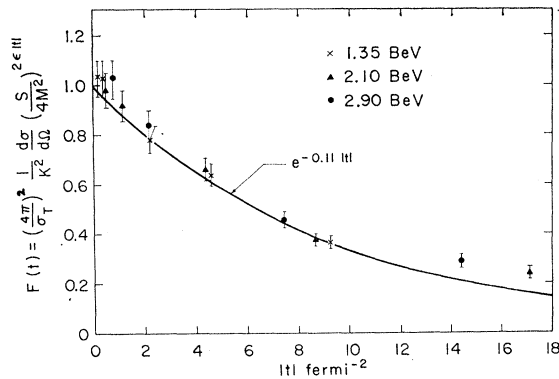


FIG. 6. Plot of a function  $F(t)$  with  $\epsilon = 1/20m_\pi^2$ .

<sup>17</sup> S. C. Frautschi (private communication).

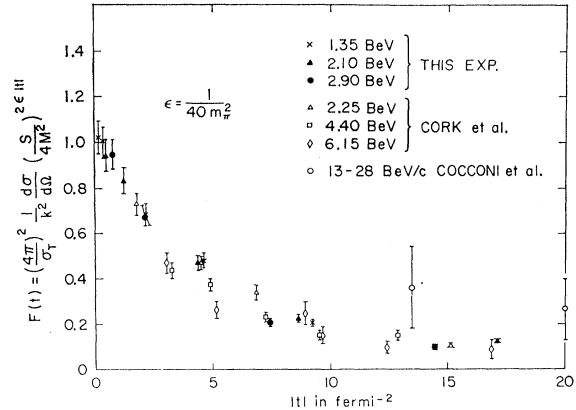


FIG. 7. Plot of a function  $F(t)$  with  $\epsilon = 1/40m_\pi^2$ .

that the next highest term to be added in Eq. (4) may be of the form  $F_2(t)(S/2M^2)^{L_1(t)+L_2(t)-2}$ , where  $L_2(t)$  corresponds to the trajectory passing through either the  $\eta^0$  or  $\omega^0$  particle. However, the variation of cross sections with energy in our data was not sensitive enough to evaluate this second term.

#### ACKNOWLEDGMENTS

The authors wish to express their gratitude to Professor S. C. Frautschi and Dr. M. Froissart for valuable discussions concerning the application of the composite particle theory to our data and to Professor G. Cocconi for first bringing this theory to our attention. We are also indebted to the staff and crew of the Cosmotron Department for their effective operation and generous assistance during the experiment.